

Glycometallate surfactants. Part 1: non-aqueous synthesis of mesoporous silica

Deepa Khushalani,^a Geoffrey A. Ozin^{*a} and Alex Kuperman^{*b}

^aMaterials Chemistry Research Group, Lash Miller Chemical Laboratories, 80 St. George Street, University of Toronto, Toronto, Ontario, Canada M5S 3H6

^bThe Dow Chemical Company, Corporate R&D, 1776 Bldg., Midland, Michigan, 48674, USA

Received 23rd March 1999, Accepted 6th May 1999

A novel two step procedure for the synthesis of hexagonal mesoporous silica has been developed. The first non-aqueous step involves the use of ethylene glycol both as solvent and chelating alkoxide. In this step a cetyltrimethylammonium glycosilicate(IV), $\text{CTA}_2[\text{Si}_2(\text{OCH}_2\text{CH}_2)_5]$, building-block is synthesized under non-aqueous conditions by solubilizing SiO_2 with NaOH in ethylene glycol in the presence of CTACl. Alternatively, $\text{CTA}_2[\text{Si}_2(\text{OCH}_2\text{CH}_2)_5]$ can be formed by reacting sodium glycosilicate(IV), $\text{Na}_2[\text{Si}_2(\text{OCH}_2\text{CH}_2)_5]$, with CTACl under non-aqueous conditions in ethylene glycol. The glycosilicate(IV) is a structurally well defined dimeric anion based on trigonal-bipyramidal silicon(IV) containing two bidentate and one bridging monodentate glycolate ligand. In ethylene glycol the glycosilicate(IV) surfactant $\text{CTA}_2[\text{Si}_2(\text{OCH}_2\text{CH}_2)_5]$ self-assembles into a lamellar mesophase containing bilayers of cationic CTA^+ that are charge-balanced by $[\text{Si}_2(\text{OCH}_2\text{CH}_2)_5]^{2-}$ counter-anions. In the second step of the preparation, controlled hydrolysis of the lamellar glycosilicate(IV) phase with water leads to a well ordered hexagonal mesoporous silica in which the extent of condensation-polymerization of the silica is insufficient to sustain the integrity of the structure when the CTA^+ cation is removed from the channels. Structure re-enforcement can however be achieved by various post-treatments of the vacuum dehydrated mesoporous silica that enable the creation of stable silica-based mesoporous materials with a wide range of elemental compositions. In this paper a post-treatment with Si_2H_6 at 100°C was employed to produce extensively polymerized hexagonal mesoporous silica that is stable to removal of the surfactant. The method described in this paper is a novel approach to the synthesis of stable and structurally well defined mesoporous silica-based materials with a wide range of elemental compositions.

Introduction

In 1992, researchers at Mobil Technology Company published the first report of organized inorganic oxide-based mesostructured materials.^{1,2} The materials were built of amorphous silica and the templating agent was a self-assembled supramolecular aggregate of amphiphilic molecules. They were denoted as the MCM41S family of materials and specifically, MCM-41 was referred to as the phase which contained hexagonally closed packed cylindrical channels. The MCM41S family of materials have high surface areas ($> 1000 \text{ m}^2 \text{ g}^{-1}$) and impressive monodispersed mesoporosity which is found to be ordered and tunable in the range of 20 to 100 Å. These materials are typically synthesized from aqueous mixtures containing a source of silica and a surfactant template under appropriate conditions of pH, temperature and time. The synthesis process was postulated to involve the formation and condensation-polymerization of a silicate liquid crystal. Although the details of this are still the subject of ongoing debate the mode of formation can nonetheless be summarized to entail electrostatic interactions between a supramolecular assembly of charged amphiphilic templates and soluble silicate species. Under base- or acid-catalyzed reaction conditions the silicates undergo polymerization to form, in most cases, a thermally stable and ordered mesoporous silica.

In this paper we present a novel non-aqueous approach to the synthesis of mesoporous silica. It involves *in situ* formation of a glycosilicate(IV) precursor that self-assembles with CTABr surfactant into a supramolecular lamellar mesophase in the ethylene glycol solvent. In a subsequent step this mesophase is hydrolyzed under controlled conditions of pH and temperature to form the desired hexagonal mesoporous silica phase.

Non-aqueous assembly of CTABr

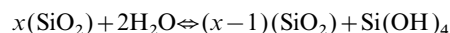
Surfactant self-assembly in non-aqueous solutions has been widely investigated both experimentally and theoretically.

There has been a need to determine their behavior in media other than water in order to improve the understanding of the mechanism of aggregate formation. In water, properties such as the electrical conductivity, surface tension, solubilization capacity and light scattering intensity as a function of the total surfactant concentration show a sharp transition in the value of the measured property over a very narrow range of surfactant concentration known as the critical micellization concentration (cmc). However, significantly different behavior is observed when the surfactant molecules are dissolved in non-aqueous solvents. The aggregates formed are usually found to be smaller and the solution properties change only gradually as a function of the surfactant concentration, thus making the experimental identification of cmc somewhat ambiguous.^{3,4}

Specifically, abundant literature exists for ethylene glycol that cites the behavior of various types of surfactants which can be solvated in this polar organic solvent.⁵⁻⁷ For cetyltrimethylammonium bromide (CTABr) it can be surmised that irrespective of the exact concentration it is still capable of aggregating and behaving as an amphiphilic molecule, albeit the region over which the various liquid-crystal phases exist is small. Table 1 provides comparative data for CTABr in water and ethylene glycol.

Silica and its behavior in ethylene glycol

In water, the solubility of silica is governed by the hydration-dehydration equilibrium:



The use of non-aqueous solvents changes the solubility of silica depending on the solvent and the type of silica. In addition, the rate of dissolution also depends on catalysts present as the forward reaction is catalyzed by anions such as hydroxide, fluoride or molybdate. Organic compounds can

Table 1 Physical data for water and ethylene glycol⁸

Solvent	CTABr cmc/mol dm ⁻³	Relative permittivity, $\epsilon/\text{dm}^3 \text{ mol}^{-1} \text{ cm}^{-1}$	Surface tension/mN m ⁻¹	Solubility parameter
Water	8.2×10^{-4}	78.5	72.8	47.9
Ethylene glycol	0.1	37.5	47.7	29.9

either retard dissolution by covering the silica surface with a strongly sorbed film or accelerate dissolution by removing the soluble Si(OH)₄ that is in equilibrium with the surface and converting it to a soluble complex.⁹

Specifically with ethylene glycol, Laine and co-workers reported in 1991¹⁰ the formation of a soluble organosilicon complex in which the ethylene glycol was chelated to a 5-coordinate silicon centre.^{10–14} The authors described a base mediated reaction in which silica was reacted with ethylene glycol and an alkali metal hydroxide with the following molar ratios: 1 SiO₂:1 MOH:40 HOCH₂CH₂OH, where M was either Cs, Na, K or Li. Under an inert atmosphere, the mixture was refluxed and the excess glycol and water produced during the course of the reaction distilled off. The resultant white product was recovered with acetonitrile and was found to be either a dimeric or a monomeric complex depending on the alkali metal used. Subsequently, Klinowski and co-workers have shown the importance of glycosilicate(IV) intermediates in the non-aqueous synthesis of zeolites, such as ZSM-5 and silica-sodalite.^{15,16}

Layered phase of mesostructured silica

Synthesis

Reagents for the synthesis were used as supplied. They included SiO₂ (Cab-O-Sil), NaOH, CTABr (Aldrich) and ethylene glycol (Aldrich, 99.0%). Ground sodium hydroxide (2.1 g, 2.2 mol) was dissolved in ethylene glycol (50 ml, 36 mol) by heating to *ca.* 100 °C. To this clear solution, cetyltrimethylammonium bromide (5 g, 1.1 mol) was added and dissolved. Finally, amorphous silica (1.5 g, 1 mol) was gradually added, while stirring. The resultant cloudy gel was aged at 80 °C for 5 days in a closed polypropylene container. To recover the product after aging, the clear viscous gel was cooled to room temperature, during which time it solidified. The product was slowly stirred into *ca.* 400 ml of de-ionized water and allowed to age at room temperature for a further 4 hours. The precipitated white powder was recovered by filtration and washed with de-ionized water to remove excess surfactant.

Results

The powder X-ray diffraction pattern of the product is shown in Fig. 1. This pattern has been indexed to a layered phase and up to 5 orders of diffraction can be easily observed, attesting to the high degree of registry of the constituent lamellae. The TGA trace of the same material is displayed in Fig. 2. Two main transitions are evident. The lower temperature transition at *ca.* 80–100 °C has been assigned to the loss of adsorbed water (5–10 wt.%) while the single transition at *ca.* 200 °C can be assigned to the decomposition of the imbibed surfactant as well as some occluded ethylene glycol. The net weight loss from this thermal transition was determined to be 75 wt.%. These values are comparable to data for the layered phase of mesoporous silica synthesized by the well studied aqueous route.^{1,2}

Formation of the hexagonal phase of mesostructured silica

Synthesis

The layered phase from the previous step was hydrolyzed with water at 80 °C. Specifically, for 1 g of the layered material

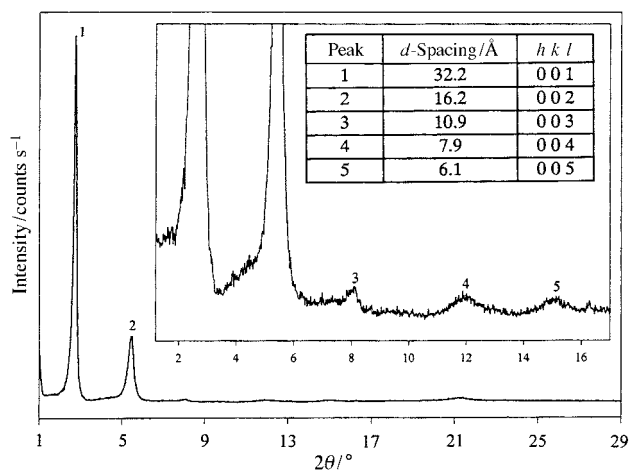


Fig. 1 PXRD pattern of the layered phase of mesostructured silica.

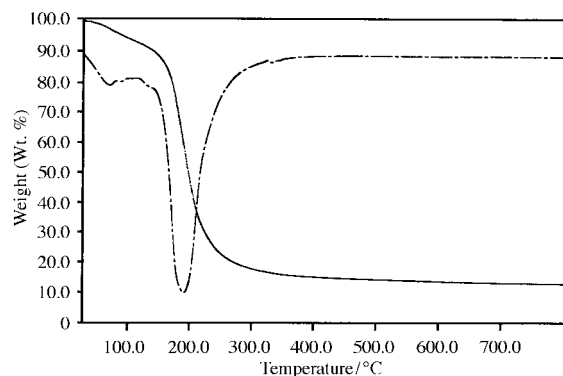


Fig. 2 TGA and derivative trace of the as-synthesized layered phase of mesostructured silica.

obtained, *ca.* 0.5 g of de-ionized water was added. The mixture was loaded into a polypropylene container and aged at 80 °C for 3 days. The ensuing product was cooled to room temperature and washed with copious amounts of de-ionized water.

Results

The PXRD pattern of the product and that of the original layered phase are shown in Fig. 3. It can be seen that the product is no longer layered. The pattern can be easily indexed to a hexagonal unit cell with $a = 44 \text{ \AA}$. The conversion of the layered mesostructured silica material to the hexagonal mesoporous silica phase was also observed by SEM and TEM, Fig. 4, 5. The SEM image clearly depicts the textural change that occurs upon the conversion. The flat 'plate' shaped moieties of the layered phase seem to stack together and a 'worm' shaped morphology results (note that the 'worm' morphology is commonly associated with the hexagonal mesoporous silica phase). This implies that a considerable amount of restructuring occurs within the silicate layers so that the channels of the mesoporous phase run along the length of the 'worms' and perpendicular to the silicate layers of the original layered phase. This contrasts with the mechanism of restructuring for the layered silicate kanemite, NaHSi₂O₅·3H₂O, into the mesoporous silica phase that was proposed by Toyota researchers.¹⁷

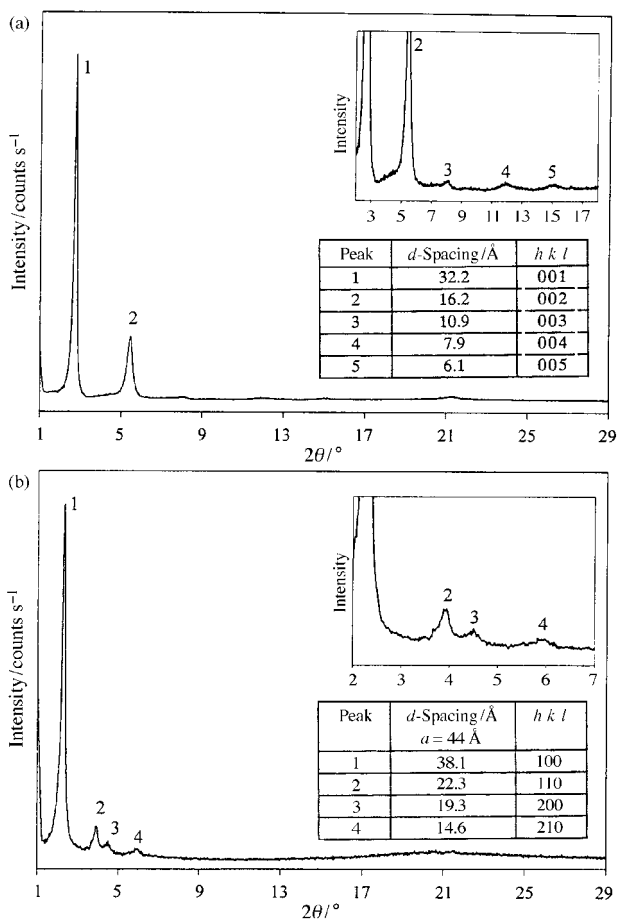


Fig. 3 PXRD patterns of (a) the layered phase and (b) the hexagonal phase of mesoporous silica obtained after hydrolysis in H₂O for 3 days at 80 °C.

²⁹Si MAS NMR data for the layered and hexagonal phases are shown in Fig. 6. The Q₄/Q₃ ratio is found to increase upon structure-conversion. For the layered phase, after fitting the spectra, the ratio was found to be 0.7 while for the hexagonal phase the ratio obtained was 1.1.

Structure reinforcement and element substitution

Synthesis

Calcination of the as-synthesized mesoporous silica material under normal conditions (increase in temperature at a rate of 1 °C min⁻¹, reaching a maximum of 540 °C) resulted in the collapse of the structure indicating an insufficient degree of silica polymerization and therefore lack of structural integrity upon removal of the template. Notably, the high concentration of hydroxyl defects in the structure creates optimum conditions for the incorporation of a large variety of elements into the walls of the mesoporous silica, allowing tailoring of chemical and physical properties as well as control of pore size. It should be noted here that elemental structure substitution may be performed during the hydrolysis step using the appropriate reagents, such as metal alkoxides.

In the work described in this paper, in order to improve the structural stability of the as-synthesized mesoporous silica material, the following treatment was performed. First, the sample was dehydrated at 100 °C under vacuum for 3–5 h in a quartz cell. Following this, Si₂H₆ (disilane, Johnson Matthey, 98% purity, used as supplied) was slowly added to the cell at room temperature. The amount of Si₂H₆ added was followed gravimetrically and varied from 7 wt.% to 12 wt.% of the total weight depending on the sample. The mixture of the sample with Si₂H₆ was then heated to 100 °C and maintained at 100 °C

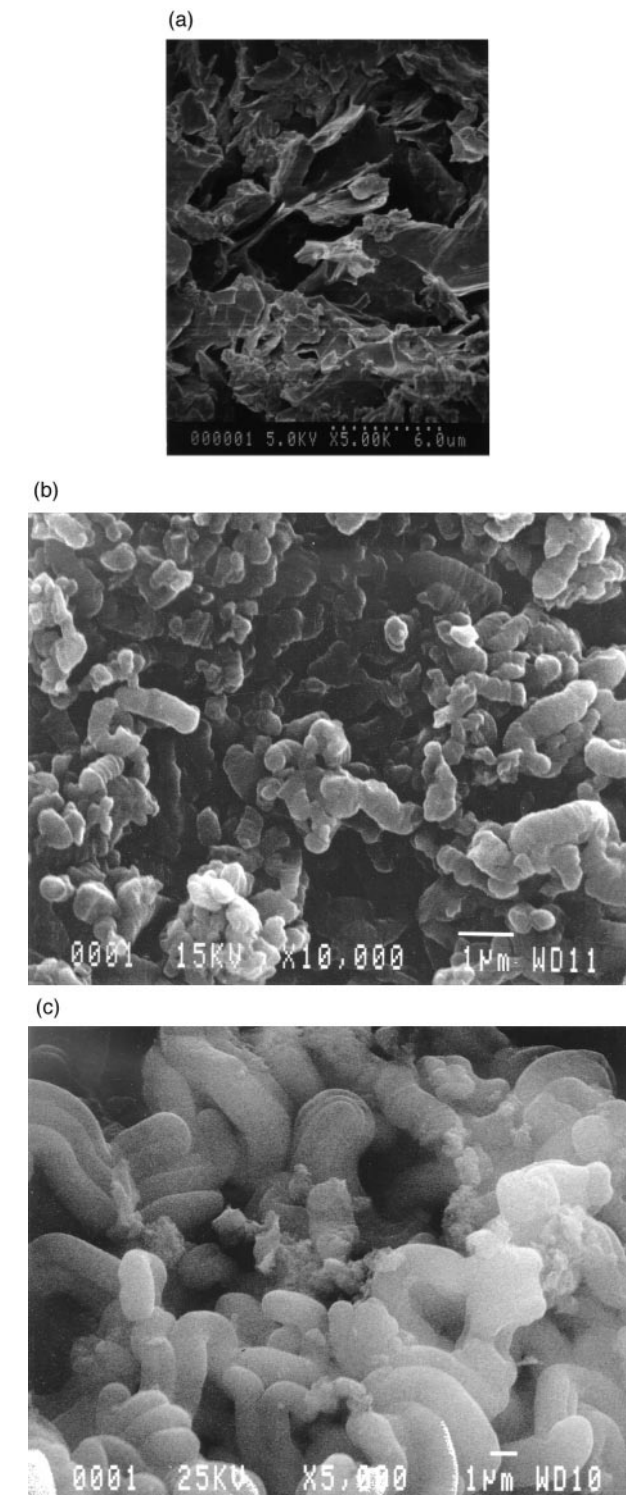


Fig. 4 SEM micrographs displaying the changes in morphology in converting (a) the layered phase of mesostructured silica to (b) the hexagonal phase of mesoporous silica and then (c) after disilane deposition.

for 24 hours in the closed cell. Following this treatment, excess unreacted Si₂H₆ was pumped out and the sample was slowly exposed to air. The product was calcined in air at 540 °C using a 1 °C min⁻¹ ramp.

Results

The PXRD patterns of the Si₂H₆ treated samples are shown in Fig. 7. Upon Si₂H₆ treatment the *d*₁₀₀-spacing of the as-synthesized mesoporous silica material decreases by ca. 5 Å along with a corresponding increase in the absolute intensity

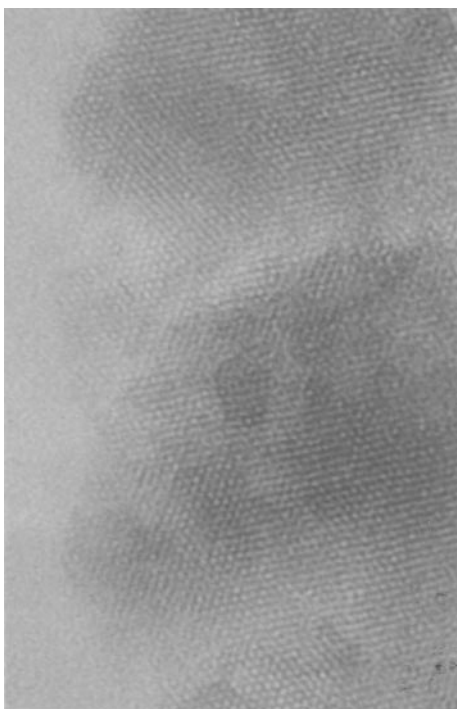


Fig. 5 TEM micrograph of the cross-sectional view of the hexagonal pore structure obtained after converting the layered phase of mesostructured silica. Magnification bar = 32 nm.

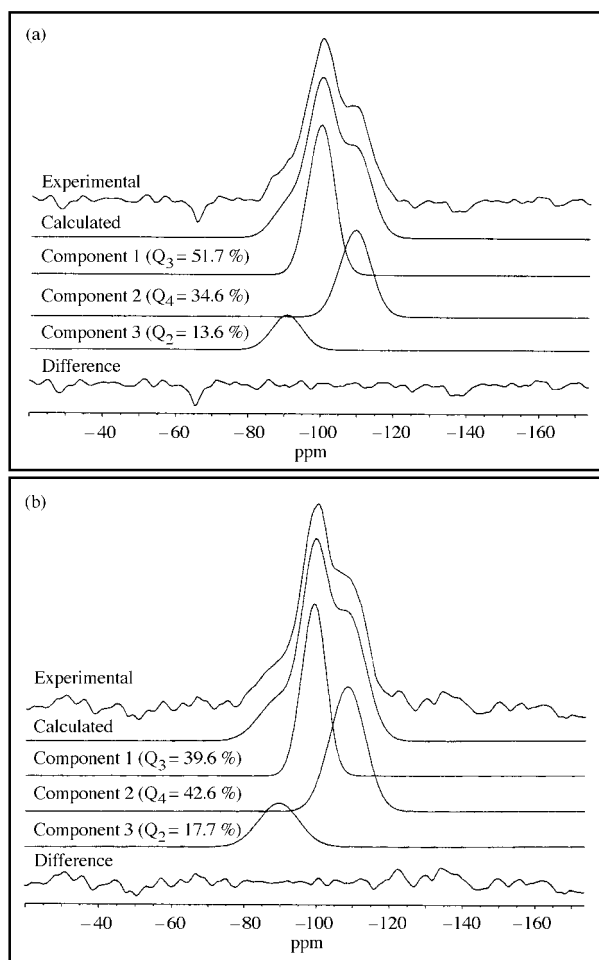


Fig. 6 ^{29}Si MAS NMR spectra (experimental and calculated) of (a) the layered phase of mesostructured silica, $Q_4/Q_3=0.7$, and (b) the hexagonal phase of mesoporous silica, $Q_4/Q_3=1.1$.

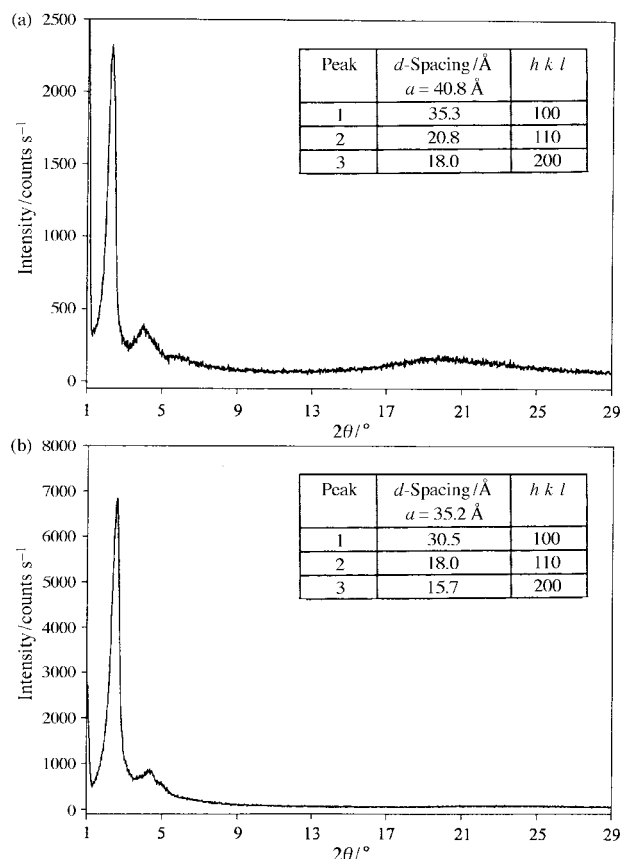


Fig. 7 PXRD patterns of (a) as-synthesized disilane treated hexagonal phase of mesoporous silica and (b) after calcination.

of the peaks. The decrease in the unit cell parameter a can be attributed to the condensation of the silanol groups in the channel walls concomitant with the removal of the surfactant template from the channels. As for the increase in intensity of the peaks, this is usually characteristic of an increase in the spatial ordering of the pores in the mesostructure that occurred upon the silanation and thermal treatment.

A comparison of the SEM images for the layered, hexagonal and Si_2H_6 treated phases of mesostructured silica is shown in Fig. 4. Morphological changes are apparent and include an increase in the smoothness of the surface of the 'worm' shaped structures along with an increase in their actual size. ^{29}Si MAS NMR spectra are shown in Fig. 8. It is interesting to note that the sample after Si_2H_6 treatment has a broad peak in the NMR spectrum centered at *ca.* -110 ppm along with a smaller peak at -85 ppm. Although the broad peak can be assigned to the various Q_n environments, the one at -85 ppm is assigned to silicon hydrides that must exist due to incomplete disilane reactions that occur during the silanation treatment. Upon calcination this peak is no longer observed in the spectrum. The fitting of the NMR spectrum of the calcined sample, in which the Q_n signals are better resolved, provided a Q_4/Q_3 ratio of higher than 3, indicating an extremely well polymerized framework.

Discussion

Based on the data presented in this paper, the reaction pathway for the formation of the mesoporous silica phase is as follows. During the first stage of the synthesis the silica reacts with ethylene glycol to form *in situ* a stable sodium glycosilicate(IV) precursor species. These species in the presence of the cetyltrimethylammonium surfactant form a novel supramolecular sol-gel surfactant mesophase, $(\text{CTA})_2[\text{Si}_2(\text{OCH}_2\text{CH}_2\text{O})_5]$. Upon addition of water the mesophase is hydrolyzed and the

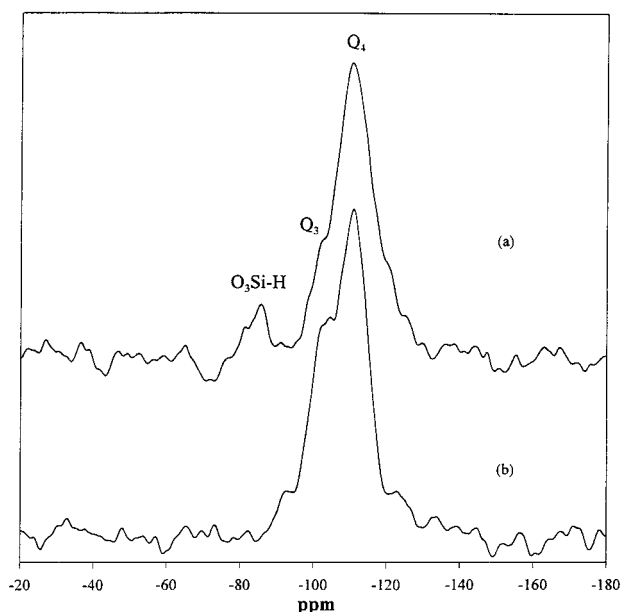


Fig. 8 ^{29}Si MAS NMR spectra of (a) hexagonal phase of mesoporous silica with Si_2H_6 deposited and (b) after calcination.

silica component undergoes condensation-polymerization to yield a layered phase of mesostructured silica. The process is represented schematically in Fig. 9. The interaction of the well defined anionic penta-coordinate silicon centers with the cationic surfactant template is believed to be pivotal in that it facilitates ordering of the co-assembly, control over the rate of hydrolysis of the glycosilicate and possibly the ensuing condensation reactions, and thus the structure of the products.

Support for the formation of the $\text{Na}_2[\text{Si}_2(\text{OCH}_2\text{CH}_2\text{O})_5]$ glycosilicate(IV) complex and the $(\text{CTA})_2[\text{Si}_2(\text{OCH}_2\text{CH}_2\text{O})_5]$ glycosilicate(IV) complex is obtained through a combination of techniques. Initially, several solvents were employed in trials for the synthesis of mesoporous silica, such as formamide, dimethylformamide and methanol. However, only ethylene glycol was able to provide a successful route to the mesolamellar silica product. This implied that the ethylene glycol played a pivotal role in the formation of reactive intermediates. Moreover, to prove that the sodium glycosilicate(IV) complex could perhaps be the intermediate, fumed silica, which serves as the source of silica in the reaction, was replaced by the previously isolated sodium glycosilicate(IV) complex. The complex was prepared according to the procedure published by Blohowiak and co-workers.¹¹ The remainder of the synthesis of the mesoporous silica material was performed in the same way as with fumed silica as the source material. The product was the same desired layered phase of mesostructured silica.

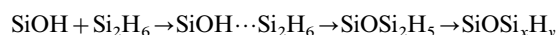
Further confirmation of the presence of the glycosilicate(IV) species was obtained by solid-state ^{29}Si MAS NMR studies. Fig. 10 displays NMR spectra of the synthesis gel that has been aged at 80°C for 5 days, prior to the condensation-polymerization reaction. Six peaks are clearly observed in the spectrum at -71.9 , -72.7 , -89.4 , -98.5 , -103.9 and -105.1 ppm. The first four peaks at -71.9 , -72.7 , -89.4 and -98.5 ppm have been assigned, according to the literature, to monomer, dimer and trimer silicate species (that is, 4-coordinate Q_1 , Q_2 and Q_3 silicate units).¹⁸⁻²¹ The other two peaks observed at -103.9 and -105.1 ppm are of special interest as they directly indicate the presence of the 5-coordinate glycosilicate(IV) species (the former is the monomer and the latter is the dimeric form of the glycosilicate(IV)).¹⁵ In fact, Klinowski and co-workers have studied the role of the sodium glycosilicate(IV) in the non-aqueous synthesis of all-silica sodalite and observed both the 5- and 4-coordinate silicon species in the synthesis mixture. They concluded that glycosil-

icate(IV) complexes start to form at approximately 50°C . The monomer, dimer and tetramer silicate species (containing 4-coordinate silicon centers) formed simultaneously. The NMR signal corresponding to these 4-coordinate silicate species decreased in intensity with increasing time and temperature, suggesting that they were actually intermediates in the synthesis of the 5-coordinate glycosilicate(IV) complex.

Following the formation of the layered mesostructured silica phase, it was converted in a second hydrolysis step at 80°C to the hexagonal mesoporous silica phase. The transformation occurs as a result of restructuring of the mesolamellar silica phase in the presence of additional amounts of water, which involves base catalyzed condensation of reactive silanol groups and re-organization of the organic templating species yielding a hexagonal mesoporous silica phase with a higher degree of silica polymerization. The NMR results showed an increase in the Q_4/Q_3 ratio for this conversion, indicating improved framework connectivity. Additional support for the proposed transformation was gained through the examination of SEM and TEM micrographs.

As the hexagonal mesoporous silica structure was found to be highly reactive and thermally unstable due to the existence of a large concentration of terminal silanols, a vapor deposition treatment involving Si_2H_6 was performed. Treatment of the as-synthesized material with a minimum of 7 wt.% of disilane resulted in an increase in the Q_4 population of the siliceous framework along with a substantial improvement in the thermal stability. The anchoring and sorption reactions were monitored through mid-IR spectroscopy, Fig. 11. Upon loading Si_2H_6 in an evacuated cell followed by thermal treatment at 100°C for 24 hours some bands in the $\nu(\text{SiH})$ region at 2245 , 2180 (shoulder) and 2092 cm^{-1} were observed. It has been well established that an increase in the number of oxygen atoms around SiH_x groups causes a high energy shift in the $\nu(\text{SiH})$ stretching frequency.^{22,23} Dag and co-workers^{24,25} have analyzed in detail the anchoring properties of disilane onto mesoporous silicas. The bands at 2245 and 2180 cm^{-1} have been assigned to O_3SiH and O_2SiH_2 surface oxide-hydride species, respectively. The assignment of the additional peak at 2092 cm^{-1} may be attributed to either OSi_2SiH or Si_3SiH species and is indicative of a clustering of silicon atoms onto the surface of the channels of the hexagonal mesoporous silica host, especially upon high loading of disilane. Solid-state ^{29}Si NMR results are in accordance with the above observation where the presence of an additional peak at -85 ppm is attributed to the $\text{O}_3\text{Si-H}$ species.²⁶ As these silicon hydrides are known to be reactive with O_2 and H_2O , they consequently disappear upon calcination, as observed by FT-IR and NMR, with a concomitant formation of silanol groups.

From the results of this work and the work of Dag and co-workers^{24,25} it can be surmised that initially Si_2H_6 anchors to the surface of the mesoporous silica host by hydrogen bonding with the surface hydroxyl groups. Possible CVD reactions of disilane with hydroxyl groups of incompletely polymerized hexagonal mesoporous silica, that ensue upon increasing temperature and aging time include (not balanced stoichiometrically):



Hydrogen is reductively eliminated as Si-O-Si linkages form along with cleavage of the Si-Si bond of the Si_2H_6 molecule. Both SiH_4 as well as Si_3H_8 are by-products of the reaction and have been observed by mass spectrometry. Si_2H_6 and SiH_4 vapor can then further react with neighboring terminal silanols and provide a pathway by which the degree of cross-linking of the framework is increased. This stabilizes the structure of mesoporous silica so that it maintains the integrity even after thermal removal of the template. It should also be noted that there is a corresponding decrease in the d_{100} -spacing of the mesoporous silica once it has been treated with Si_2H_6 . This is

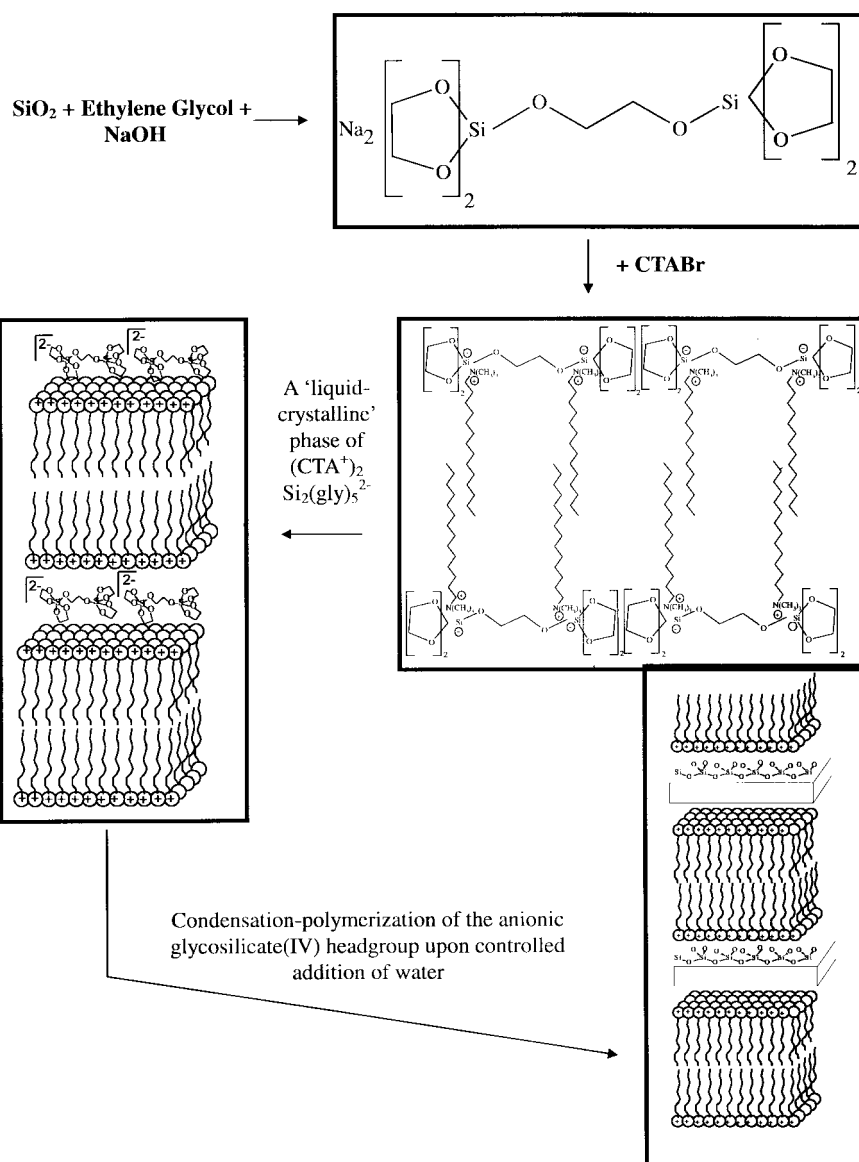


Fig. 9 Schematic representation of formation of a layered phase of mesostructured silica from silica and cetyltrimethylammonium bromide in the presence of ethylene glycol and sodium hydroxide.

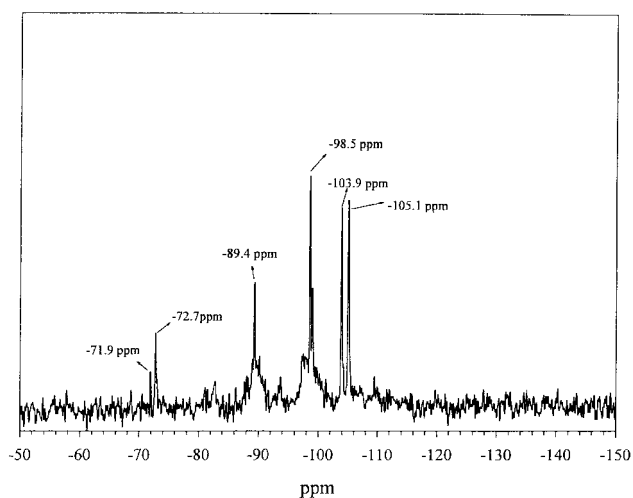


Fig. 10 ^{29}Si MAS NMR Spectrum of synthesized 'gel' before hydrolysis. Parameters used for acquisition were: 20000 scans, single pulse program with a recycle delay of 10 s, $\pi/2$ pulse width of 4.3 ms and a 5 KHz spinning speed.

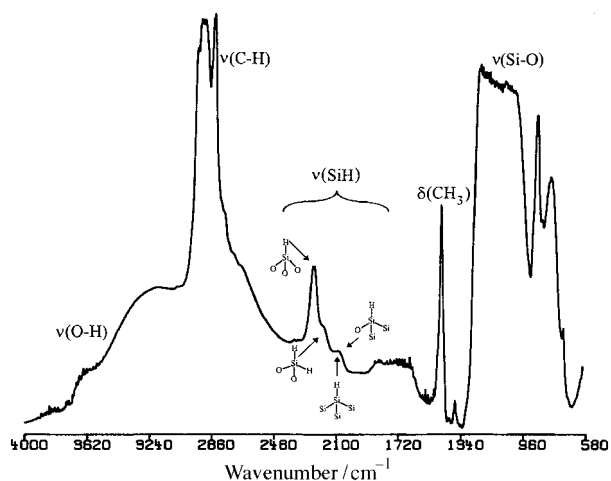


Fig. 11 FT-IR spectrum of the hexagonal phase of mesoporous silica after the reaction with disilane. Note that the sample has been exposed to air after the thermal treatment and the excess unreacted disilane has been pumped off.

consistent with the proposal that silanation treatment produces a more polymerized hexagonal mesoporous silica framework.

Conclusions

In this paper we have presented a new mild non-aqueous synthesis route to hexagonal mesoporous silica involving a novel supramolecular silicoglycolate(IV) precursor. Two phases were isolated. Initially a layered mesostructured silica phase was obtained which could be readily transformed into the hexagonal mesoporous silica phase. The hexagonal phase was structurally re-inforced by performing a CVD treatment involving disilane, Si₂H₆. This facilitated an increase in the degree of polymerization of the silica framework and allowed for removal of the surfactant template without loss of integrity of the structure.

Acknowledgements

G.A.O. is indebted to the Canada Council for the award of an Issac Walton Killam Foundation Research Fellowship (1995–97) that was held during the period of this research. G.A.O. is also deeply grateful to ESTAC and NSERC-IOR for financial support of this research.

References

- 1 C. T. Kresge, M. E. Leonowicz, W. J. Roth, J. C. Vartuli and J. S. Beck, *Nature*, 1992, **359**, 710.
- 2 J. S. Beck, J. C. Vartuli, W. J. Roth, M. E. Leonowicz, C. T. Kresge, K. T. Schmitt, C. T-W. Chu, D. H. Olson, E. W. Sheppard, S. B. McCullen, J. B. Higgins and J. L. Schlenker, *J. Am. Chem. Soc.*, 1992, **114**, 10834.
- 3 A. S. Kertes and H. Gutmann, in *Surface and Colloid Science*, ed. E. Matijevic, Interscience, New York, 1975.
- 4 E. Ruckenstein and R. Nagarajan, *J. Phys. Chem.*, 1980, **84**, 1349.
- 5 R. Nagarajan and C-C. Wang, *J. Colloid Interface Sci.*, 1996, **178**, 471 and references therein.
- 6 M. Sjöberg, U. Henriksson and T. Wärnheim, *Langmuir*, 1990, **6**, 1205.
- 7 R. Palepu, H. Gharibi, D. M. Bloor and E. Wynn-Jones, *Langmuir*, 1993, **9**, 110.
- 8 T. Wärnheim and A. Jönsson, *J. Colloid Interface Sci.*, 1988, **125**, 627.
- 9 R. K. Iler, *The Chemistry of Silica*, Wiley & Sons, New York, 1979.
- 10 R. M. Laine, K. U. Blohowiak, T. R. Robinson, M. L. Hope, P. Nardi, J. Kampf and J. Uhm, *Nature*, 1991, **353**, 642.
- 11 K. Y. Blohowiak, D. R. Treadwell, B. L. Mueller, M. L. Hoppe, S. Jouppi, P. Kansal, K. W. Chew, C. L. S. Scotto, F. Babonneau, J. Kampf and R. M. Laine, *Chem. Mater.*, 1994, **6**, 2177.
- 12 P. Kansal and R. M. Laine, *J. Am. Ceram. Soc.*, 1994, **77**, 875.
- 13 P. Kansal and R. M. Laine, *J. Am. Ceram. Soc.*, 1995, **78**, 529.
- 14 K. W. Chew, B. Dunn, T. Faltens, M. L. Hoppe, R. M. Laine, L. Nazar and H. K. Wu, *Am. Chem. Soc. Polym. Prepr.*, 1993, **34**, 254.
- 15 B. Herreros, S. W. Carr and J. Klinowski, *Science*, 1994, **263**, 1585.
- 16 B. Herreros, T. L. Barr, P. J. Barrie and J. Klinowski, *J. Phys. Chem.*, 1994, **98**, 4570.
- 17 S. Inagaki, Y. Fukushima and K. Kuroda, *J. Chem. Soc., Chem. Commun.*, 1993, 680.
- 18 N. H. Ray and R. J. Plaisted, *J. Chem. Soc., Dalton Trans.*, 1983, 475.
- 19 J. Nathan and E. Oldfield, *J. Am. Chem. Soc.*, 1985, **107**, 6769.
- 20 R. K. Harris and C. T. G. Knight, *J. Mol. Struct.*, 1982, **78**, 273.
- 21 E. Lippmaa, M. Mägi, A. Samoson, G. Engelhardt and A.-R. Grimmer, *J. Am. Chem. Soc.*, 1980, **102**, 4889.
- 22 D. Graf, S. Bauer-Mayer and A. Schnegg, *J. Appl. Phys.*, 1993, **74**, 1679.
- 23 L. Ling, S. Kuwabara, T. Abe and F. Shimura, *J. Appl. Phys.*, 1993, **73**, 3018.
- 24 E. Chomski, Ö. Dag, A. Kuperman, N. Coombs and G. A. Ozin, *Chem. Vap. Deposit.*, 1996, **2**, 8.
- 25 Ö. Dag, A. Kuperman, P. M. Macdonald and G. A. Ozin, *Stud. Surf. Sci. Catal.*, 1994, **84**, 1107.
- 26 W. K. Chang, N. Y. Liao and K. K. Gleason, *J. Phys. Chem.*, 1996, **100**, 19653.

Paper 9/02289I